



Relationship between Sentinel-2 orbital data and in situ monitoring of coffee rust

Matheus Luiz Jorge Cortez¹ · Marcelo de Carvalho Alves¹ · Gladyston Rodrigues Carvalho² · Edson Ampélio Pozza³

Received: 24 March 2020 / Accepted: 24 July 2020 / Published online: 31 July 2020
© Springer Nature Switzerland AG 2020

Abstract

Coffee rust (*Hemileia vastatrix* Berkeley & Broome) is the main coffee disease in Brazil. Coffee rust control is calendar-based and performed by applying chemicals in order to avoid the outburst of disease epidemics. The aim of this work was to identify coffee rust using multispectral orbital sensing through analyses utilising vegetation indices and coffee rust incidence, defoliation and yield data obtained in situ. Field samples were georeferenced using a high-accuracy global navigation satellite system receiver in two plots, in a 42-year-old, leaf rust susceptible coffee cultivar. Conventional chemical control of rust was performed in only one of the plots to serve as control. Coffee rust incidence in areas with and without chemical control was assessed over 5 months, from December 2018 to April 2019, a period with optimal environmental conditions for disease occurrence. Following analyses of different vegetation indices and data sampled in the coffee crop, Pearson's correlations between the variables were verified. Reported correlations occurred mainly among coffee rust incidence levels in February 2019 and vegetation indices calculated using Sentinel-2 images from August 2018, September 2018 and February 2019 [IRECI $r=0.566$; IRECI $r=0.493$; NDMI $r=-0.518$; NDVI(RE1) $r=-0.562$; CI(RE1) $r=-0.573$; MSR(RE1) $r=-0.569$], in areas without coffee rust control. Indices based on relationships between bands in the Red-Edge and Near Infra-Red regions were more sensitive to spectral changes in vegetation due to variation in coffee rust occurrence over time.

Keywords Remote sensing · Vegetation indices · Precision agriculture · Sentinel-2

1 Introduction

The coffee plant (*Coffea arabica* L.) is of great economic, social and cultural relevance in Brazil and around the world. Effective management of coffee crops can ensure good productivity, generating greater economic return, and reducing detrimental impacts to the environment.

The disease known colloquially as coffee leaf rust poses a significant threat to Brazilian coffee producers, due to favourable environmental conditions in most coffee regions of the country, and where there is still widespread use of susceptible varieties [39]. The pathogenic fungus

can cause losses of up to 50% if no control measures are employed [34, 49].

Control measures for coffee rust are administered across entire plantations, carried out with the use of protective and systemic fungicides that are applied to the plant's leaves, or by drenching the soil, respectively. Agrochemical sprayings are calendar-based starting in November/December and continuing through April [19]. The spatial and temporal distributions of coffee rust incidence are not homogeneous across a crop, thus it can be assumed that any total area leaf rust control strategy could be replaced

✉ Matheus Luiz Jorge Cortez, cortez.agro@gmail.com | ¹Agricultural Engineering Department, Federal University of Lavras, Lavras, Minas Gerais, Brazil. ²Empresa de Pesquisa Agropecuária de Minas Gerais, Epamig sul, Campus da UFLA, Lavras, Minas Gerais, Brazil. ³Plant Pathology Department, Federal University of Lavras, Lavras, Minas Gerais, Brazil.



by focused management in specific areas of disease incidence [2].

Precision agriculture techniques can result in potential benefits in profitability, yield, sustainability, crop quality and traceability, environmental protection, food security and rural economic development [35]. The efficacy of disease management strategies in the field can be accessed using geographic information system (GIS), global navigation satellite system (GNSS), geocomputation, remote sensing, and variable rate application technology integrated with advanced information processing in georeferenced maps during crop growth, development and production [3, 35].

A commonly-used remote sensing method for vegetation studies is the use of vegetation indices. Vegetation indices are mathematical operations involving two or more spectral bands designed to enhance vegetation properties, allowing reliable spatial and temporal inter-comparisons of photosynthetic activity and canopy structure [28]. The method is based on the fact that energy reflected in red and near-infrared (NIR) regions is directly related to photosynthetic activity of the vegetation canopy, as well as the assumption that using two or more spectral bands can substantially minimize the main sources of noise that affect detected variation in vegetation responses [21].

Changes observed in spectral properties within the NIR region may provide information on senescence and vegetation stress issues [31]. The Multi-Spectral Instrument (MSI) sensor embedded in the Sentinel-2 satellite obtains terrestrial surface spectral reflectance information by recording it in 13 different bands of the electromagnetic spectrum. Five of these spectral bands are positioned in distinct bands within the NIR region, and three of these five are located in the rapidly growing reflectance zone known as Red-Edge [20]. Based on reflectance measurements applied to simulate the Sentinel-2 satellite sensor bands, Chemura et al. [13] examined three levels of coffee rust severity in coffee leaves under greenhouse conditions. According to the authors, bands located at the Red-Edge spectral position can be useful for disease detection and coffee crop status evaluation.

In coffee plantations in Brazil, Landsat 7 and 8 images associated with in situ coffee rust data have been used to analyse spectral radiometry behaviour of plants under different irrigation systems [40]. The authors observed that in areas with higher coffee rust incidence under a central pivot and rainfed system, the average reflectance of NIR and green spectral regions was reduced, while reflectance increased in short wave infrared (SWIR) and red wavelengths, when compared to periods with lower coffee rust incidence. Moreover, NDVI generated by Landsat 7 ETM+ sensor images were used to evaluate coffee leaf fall caused by coffee rust in Guatemalan coffee plantations

[32]. It was observed that the NDVI standard deviation value in damaged farms increased as the average NDVI value decreased. By analysing annual NDVI changes, it was also reported that disease progression is not homogeneous in crops [32].

Based on the hypothesis that it is possible to detect changes in the spectral behaviour of plants due to the incidence of leaf rust through orbital remote sensing, this study aimed to evaluate the effectiveness of different vegetation indices for remote detection of coffee rust incidence, and to characterize the spectral signature of crops with different levels of disease incidence.

2 Materials and methods

2.1 Area description

The study area is located in Minas Gerais Agricultural Research Company (EPAMIG) experimental field in Três Pontas city, Minas Gerais state, Brazil. The cultivar present in the area is Catuaí Amarelo IAC-17, a variety susceptible to coffee rust. Plant spacing is 3.5 m × 2.0 m with 2 plants per pit, and a crop age of 42 years. The approximate central geographical point of the study area has a latitude of 21° 20' 38.36" S and a longitude of 45° 28' 48.51" W, and the average altitude is around 935 m. The region is classified as Cwa, with dry winters and rainy summers [1].

2.2 Georeferencing of sample points

Images obtained by adding the Sentinel-2 MSI sensor to the Spectra Precision SP60 L1/L2 RTK GNSS receiver software provided latitude and longitude data, corresponding to the center of fifty pixels in different spectral bands (Table 1). Subsequently, the GNSS RTK receiver base was placed in the field and the fifty sample points were manually located by walking with the mobile RTK receiver in the sampling area. In each of the fifty identified subareas (measuring 10 m × 10 m), a central coffee plant was georeferenced, which was then used to select a further two plants within a radius of approximately 2 m within the planting line. In total one hundred and fifty coffee plants were evaluated, three plants per sampling point.

2.3 Crop treatments

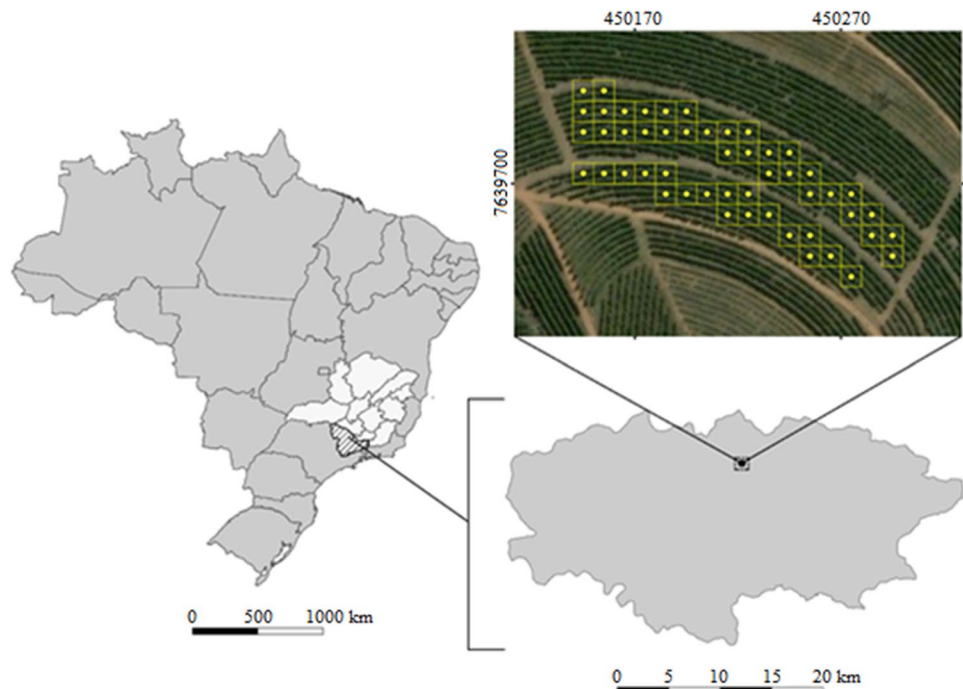
The study area was split into two sections (Fig. 1). The northern section measured approximately 0.57 ha and contained 32 sampling points, while the southern section measured around 0.43 ha and contained 18 sampling points. No rust control was performed in the northern section, however the southern section received a

Table 1 Spatial and spectral resolution of Sentinel-2 satellite MSI sensor bands [20] used to calculate vegetation indices

Sentinel-2 band	Denomination	Spectral band center (nm)	Bandwidth (nm)	Spatial resolution (m)
Coastal aerosol	B01	443	20	60
Blue	B02	490	65	10
Green	B03	560	35	10
Red	B04	665	30	10
Red Edge 1	B05	705	15	20
Red Edge 2	B06	740	15	20
Red Edge 3	B07	783	20	20
Near Infra-Red	B08	842	115	10
Near Infra-Red	B8a	865	20	20
Water vapour	B09	945	20	60
SWIR—Cirrus	B10	1375	30	60
SWIR 2	B11	1610	90	20
SWIR 3	B12	2190	180	20

systemic fungicide containing triazole and strobilurin on 11 December 2018 and 20 February 2019, as well as a leaf application of copper on 8 April 2019. The application of fertiliser was carried out following Guimarães et al. [26], based on soil fertility management and leaf nutrition in coffee culture recommended for Minas Gerais state, Brazil.

Fig. 1 Study area indicating the location of Minas Gerais state within Brazil, and the south/southwest region of the federative unit (left), the area of Três Pontas city (bottom right), and the plantation area in the EPAMIG experimental fieldsite, showing the sampling pixels (subareas) (top right)



2.4 Field evaluation: coffee rust, defoliation and yield

Coffee rust was sampled monthly between December 2018 and April 2019 (totalling five separate samples), using a non-destructive method that takes into account plant exposure to solar radiation. For each coffee plant, eight leaves were evaluated; four leaves from different randomly selected plagiotropic branches on the north-facing side of the plant (i.e. higher insolation levels), and four leaves from different plagiotropic branches on the south-facing side of the plant (lower insolation levels) [15]. Therefore, a total of 24 leaves were evaluated per subarea. Leaves of the 3rd and 4th pair of plagiotropic branches in the middle third of the plants were assessed according to the methodology proposed by Lima [36]. The percentage of coffee rust incidence for each subarea was obtained by dividing the total number of leaves with recorded coffee rust signals by the total number of leaves evaluated in the subarea (24 leaves), and multiplied by one hundred.

Defoliation was determined using strands positioned at two points on one plagiotropic branch of each of the one hundred and fifty coffee plants. Leaf fall was recorded in each monthly assessment following the initial number of leaves counted in December 2018, totalling five samples. These leaf drop data were then transformed into a percentage of defoliation.

Fruit harvest was carried out on 2 July 2019 with a portable Nakashi DL 262-MT2L[®] gasoline machine. A cloth was placed on the floor around the plants to facilitate the

collection of the fallen fruits. The volume of fruits from the three plants in each subarea was measured using a graduated bucket, meaning that the volume assigned to each of the fifty subareas corresponded to liters per three plants. Fruits were collected from all one hundred and fifty plants that were previously evaluated for coffee rust incidence levels.

2.5 Multispectral data

The orbital data captured by the Sentinel-2 satellite-embedded MSI sensor was obtained by a free download available from the United States Geological Survey [44] collection. Sentinel-2 scenes were selected using the criteria of least atmospheric interference and closest proximity to date of crop rust sampling (Table 2).

2.6 Sentinel-2 digital image processing

Digital images were processed using the Dark Object Subtraction (DOS) method [11, 12]. Correction by the DOS method is carried out by estimating the atmospheric interference in each spectral band, performing calculations to

transform the digital number into radiance values, and then to surface reflectance values. Minimum and maximum radiance, top-level irradiance, and sensor gain were necessary variables for calculations, and varied for different bands. Additionally, other factors that depend on the image date were included, such as Earth-Sun distance and solar elevation angle [27].

2.7 Vegetation indices calculations and Pearson’s correlations

Vegetation indices (Table 3) using different relationships between Sentinel-2 spectral bands were calculated. The vegetation indices selected provide data on plant canopy such as leaf area, plant leaf moisture and chlorophyll content.

Vegetation index calculations (Table 3) were performed for 7 selected Sentinel-2 images for correlation with coffee rust incidence, defoliation and yield data. Another Sentinel-2 image (November 2018) was selected for index calculations for use in comparison with monthly rainfall intensity data. To perform the correlations, values were extracted from each index corresponding to the 50

Table 2 Dates that in situ data were obtained, respective orbital data used for correlation analysis and cloud coverage of Sentinel-2 images [44]

Data	August	September	November	December	January	February	March	April
In situ	–	–	–	2018/12/14	2019/01/14	2019/02/15	2019/03/15	2019/04/19
Orbitals	2018/08/20	2018/09/09	2018/11/28	2018/12/13	2019/01/17	2019/02/01	2019/03/08	2019/04/22
Cloud cover (%)	< 10	< 10	< 10	< 10	< 20	< 10	< 10	< 10

Table 3 Vegetation indices calculated to correlate with leaf rust incidence, defoliation and yield data obtained from field samples, spectral bands necessary for index calculations and authors who developed/adapted them

Index	Formula	Source
Normalized Difference Vegetation Index	$NDVI = \frac{(B8-B4)}{(B8+B4)}$	Rouse et al. [42]
Normalized Difference Moisture Index (B11)	$NDMI(B11) = \frac{(B8-B11)}{(B8+B11)}$	Wilson and Sader [46]
Normalized Difference Moisture Index (B12)	$NDMI(B12) = \frac{(B8-B12)}{(B8+B12)}$	Wilson and Sader [46]
Renormalized Normalized Difference Vegetation Index	$RNDVI = \frac{(B8-B4)}{\sqrt{B8+B4}}$	Gitelson and Merzlyak [23]
Inverted Red-Edge Chlorophyll Index	$IRECI = \frac{(B8-B4)}{\sqrt{B6/B5}}$	Frampton et al. [22]
Normalized Difference Vegetation Index (RE1)	$NDVI(RE1) = \frac{(B8-B5)}{(B8+B5)}$	Gitelson and Merzlyak [23]
Red-Edge Chlorophyll Index	$CI(RE1) = (B8/B5) - 1$	Gitelson et al. [24]
Transformed Chlorophyll Absorption Ratio Index/Optimized Soil-Adjusted Vegetation Index	$\frac{TCARI}{OSAVI} = \frac{3 * [(B6-B5) - 0.2 * (B6-B3)] * (B6/B5)}{[(1+0.16) * (B6-B5)] / B6 + B5 + 0.16}$	Rondeaux et al. [41], Daughtry et al. [17], Wu et al. [47]
Modified Chlorophyll Absorption Ratio Index/Optimized Soil-Adjusted Vegetation Index	$\frac{MCARI}{OSAVI} = \frac{[(B6-B5) - 0.2 * (B6-B3)] * (B6/B5)}{[(1+0.16) * (B6-B5)] / B6 + B5 + 0.16}$	Rondeaux et al. [41], Daughtry et al. [17], Wu et al. [47]
Modified Simple Ratio (RE1)	$MSR(RE1) = \frac{[(B8/B5) - 1]}{\sqrt{(B8/B5) + 1}}$	Chen [14], Wu et al. [47]

georeferenced subareas in the coffee crop area selected for rust sampling (i.e. the 50 pixels of highest spatial resolution bands of Sentinel-2 MSI images). Pearson's correlations (Fig. 2) were performed between in situ data and vegetation indices values extracted from the 18 sampling points in the southern section (with coffee rust chemical control). The same procedure was performed for the 32 points in the northern section (without coffee rust chemical control).

In order to evaluate spectral behaviour in the south and north sections, reflectance values of each 50 sample points were extracted from all 13 spectral bands in the Sentinel-2 images. For each of the 13 bands, monthly mean reflectance values of the 32 northern sample points were calculated. The same procedure was performed for the 18 southern sample points. Student's *t*-tests were then performed to compare monthly averages of areas with and without leaf rust chemical control.

2.8 Meteorological in situ data

To better understand the coffee plant's spectral response to coffee rust, monthly rainfall data were used to compare with the monthly vegetation indices data. Rainfall intensity (mm/month) was measured with a rain gauge from three conventional weather stations located in the cities of Machado, Lavras and São Lourenço, that surround the EPAMIG experimental fieldsite in Minas Gerais state, Brazil [30]. With these data, rainfall intensity interpolation was performed by using an inverse distance weighting method [45].

3 Results

3.1 Spatial-temporal coffee rust distribution

An increase in coffee rust incidence was recorded over the months of assessment, most notably in the area where the disease was not controlled (Fig. 3). Coffee rust incidence classes were defined in order to facilitate the visualization of rust spatiotemporal progress (Fig. 4).

3.2 Correlation of data derived from Sentinel 2 with field data

Pearson's correlation indicated an interaction between levels of coffee rust incidence and the vegetation indices

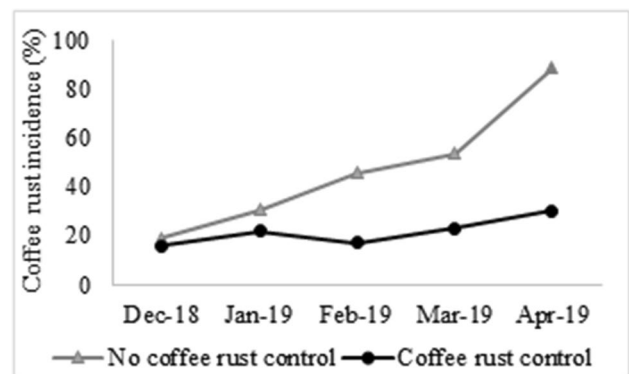


Fig. 3 Coffee rust incidence percentage between December 2018 and April 2019 in areas with and without chemical control in the EPAMIG experimental fieldsite, Três Pontas city, Minas Gerais state, Brazil

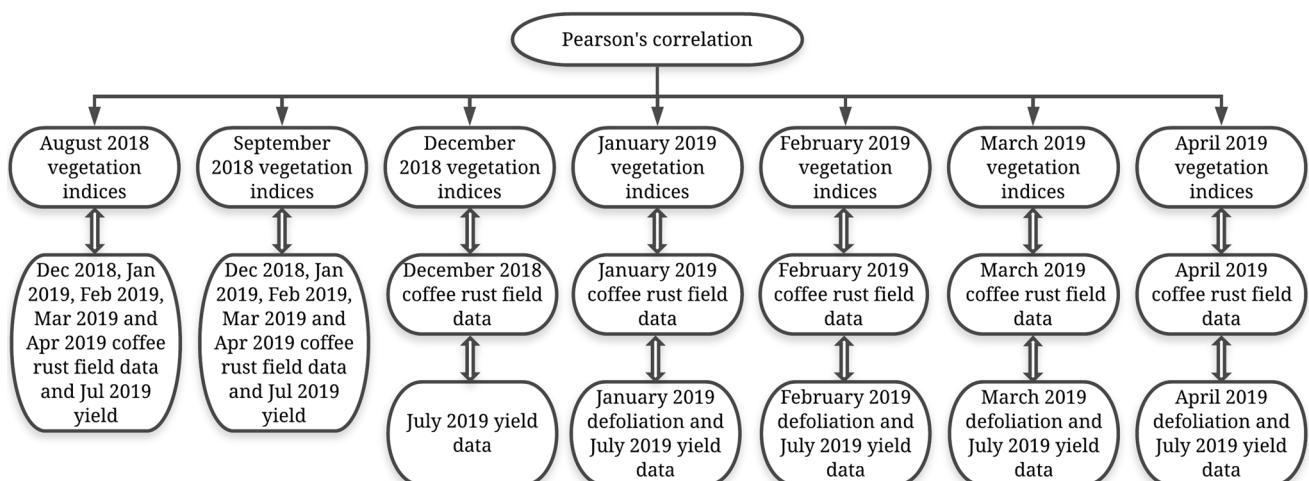


Fig. 2 Correlations between field data sampled in EPAMIG experimental fieldsite in Três Pontas city and vegetation indices calculated with Sentinel-2 images

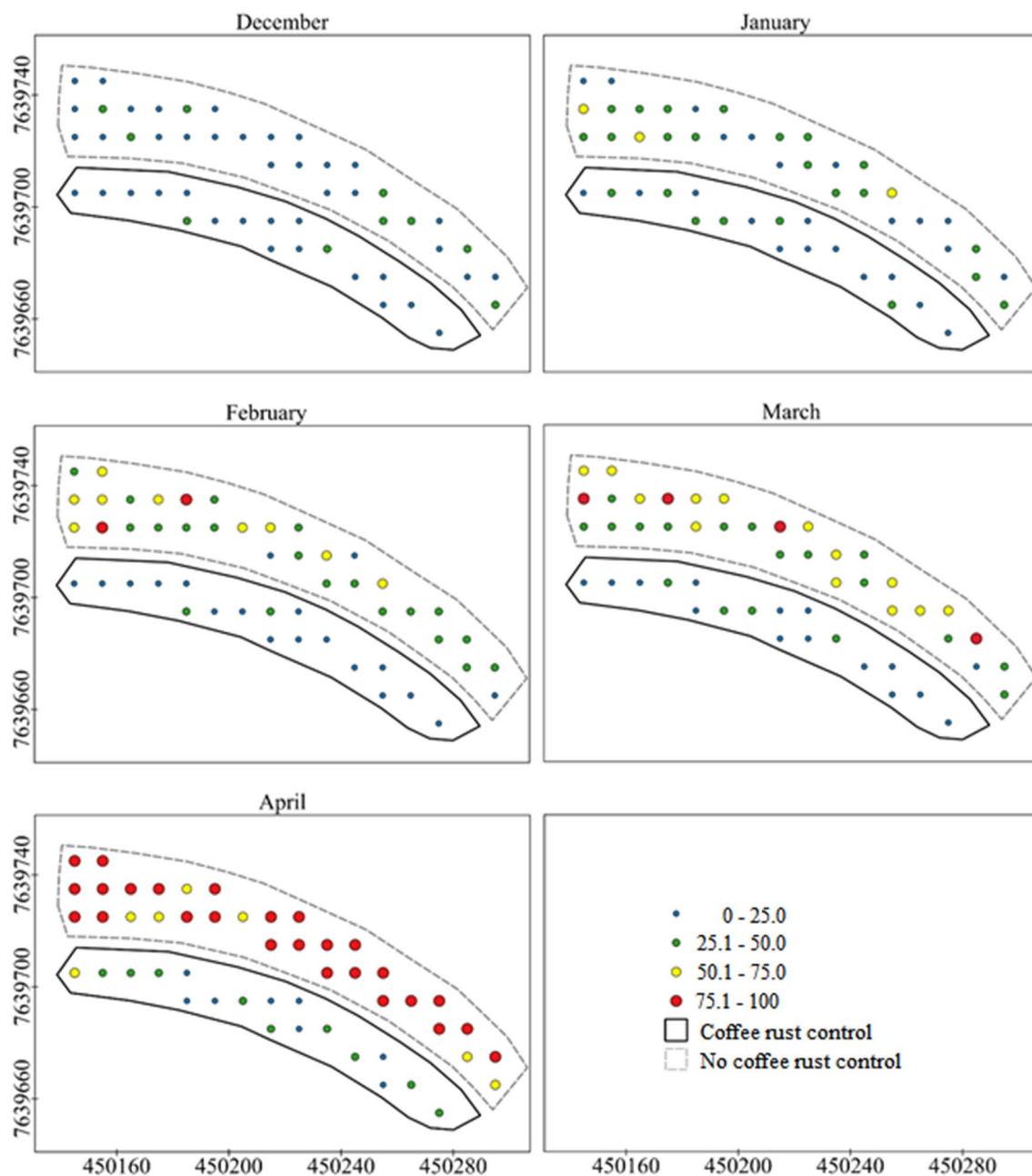


Fig. 4 Coffee rust incidence percentage in crop subareas over time in control and uncontrolled sections (continuous and dashed lines, respectively) in the EPAMIG experimental fieldsite, Três Pontas city, Minas Gerais state, Brazil

calculated for each respective month of evaluation. It was noted that in February 2019 negative correlations were reported between various vegetation indices and coffee rust incidence in the northern section of the study site (Table 4).

The vegetation indices calculated with the February 2019 images using spectral bands in NIR (B08) and Red-Edge 1 (B05) presented the highest correlation values with leaf rust data sampled in the respective month [NDVI(RE1) $r = -0.562$; CI(RE1) $r = -0.573$; MSR(RE1) $r = -0.569$]. For

NDMI indices calculated using NIR band (B08) and one of the bands in SWIR position (B11 or B12), we obtained, respectively, moderate and weak correlations for February 2019 ($r = -0.518$ and $r = -0.481$), and moderate for April 2019 ($r = -0.502$ and $r = -0.519$).

The yield harvested in July 2019 had a moderate positive correlation ($r = 0.555$) with coffee rust incidence reported in April 2019 in the sampling section without any chemical control. Furthermore, the IRECI vegetation index generated from images recorded in August and

September 2018 also correlated positively with leaf rust assessment data obtained in February and March 2019 (Tables 5 and 6).

3.3 Reflectance and vegetation index averages in areas with and without coffee rust control

By analysing average monthly reflectances for the different bands of the electromagnetic spectrum in both

Table 4 Pearson’s correlations (r) between different vegetation indices, yield and defoliation coffee rust incidence between December 2018 and April 2019, in sampling areas with chemical control measures (c), and without chemical control measures (nc)

Data	Dec (nc)	Dec (c)	Jan (nc)	Jan (c)	Feb (nc)	Feb (c)	Mar (nc)	Mar (c)	Apr (nc)	Apr (c)
YIELD	-0.132	-0.390	-0.291	-0.406	-0.082	-0.173	0.243	0.034	0.555	0.307
DEFOLIATION	-	-	0.384	0.113	0.230	0.030	0.220	0.116	0.268	0.131
NDVI	-0.173	-0.316	-0.036	-0.295	-0.313	0.251	-0.166	-0.001	0.257	-0.435
NDMI(B11)	0.077	-0.292	-0.039	-0.451	-0.518	-0.007	-0.266	-0.078	0.122	-0.502
NDMI(B12)	0.116	-0.218	-0.100	-0.450	-0.481	-0.039	-0.175	0.007	0.092	-0.519
RNDVI	-0.132	-0.338	-0.033	-0.375	-0.426	0.236	-0.288	-0.087	0.242	-0.448
IRECI	-0.211	-0.360	0.262	0.039	-0.124	0.210	-0.040	-0.249	0.155	-0.361
NDVI(RE1)	0.193	-0.212	-0.178	-0.403	-0.562	0.031	-0.378	-0.037	0.133	-0.461
CI(RE1)	0.199	-0.220	-0.182	-0.401	-0.573	0.034	-0.371	-0.034	0.137	-0.426
TCARI/OSAVI	-0.078	0.201	0.189	0.310	0.473	-0.127	0.269	-0.087	-0.219	0.445
MCARI/OSAVI	0.220	-0.127	-0.154	-0.283	-0.474	-0.050	-0.385	0.019	0.135	-0.359
MSR(RE1)	0.197	-0.217	-0.181	-0.402	-0.569	0.033	-0.374	-0.035	0.135	-0.440

Significant r values ($p < 0.05$) are in bold

Table 5 Pearson’s correlations (r) between vegetation indices calculated with August images with coffee rust incidence data and yield data from sample points in the area without chemical control

August indices	Dec	Jan	Feb	Mar	Apr	Yield
NDVI	0.041	-0.019	0.221	0.246	0.054	-0.134
NDMI(B11)	0.013	-0.112	-0.114	0.241	0.137	0.090
NDMI(B12)	-0.058	-0.219	-0.143	0.236	0.060	0.171
RNDVI	0.080	-0.023	0.266	0.304	0.114	-0.096
IRECI	0.138	0.024	0.566	0.447	0.193	-0.062
NDVI(RE1)	0.010	-0.166	-0.262	0.096	0.056	0.051
CI(RE1)	0.016	-0.147	-0.240	0.102	0.077	0.058
TCARI/OSAVI	0.011	0.052	0.169	-0.090	-0.081	0.011
MCARI/OSAVI	0.029	-0.038	-0.477	-0.209	-0.021	-0.007
MSR(RE1)	0.013	-0.155	-0.249	0.100	0.068	0.055

Significant values ($p < 0.05$) are in bold

Table 6 Pearson’s correlations (r) between vegetation indices calculated with September images with coffee rust incidence data and yield data from sample points in the area without chemical control

September indices	Dec	Jan	Feb	Mar	Apr	Yield
NDVI	0.021	-0.064	0.120	0.194	0.068	-0.100
NDMI(B11)	0.036	-0.077	-0.118	0.235	0.171	0.069
NDMI(B12)	-0.031	-0.060	-0.165	0.190	0.090	0.019
RNDVI	0.057	-0.033	0.198	0.249	0.118	-0.100
IRECI	0.097	0.027	0.493	0.389	0.256	-0.074
NDVI(RE1)	0.051	-0.121	-0.204	0.040	-0.010	0.036
CI(RE1)	0.059	-0.131	-0.205	0.053	0.018	0.063
TCARI/OSAVI	-0.002	0.135	0.131	-0.110	0.009	0.035
MCARI/OSAVI	0.042	0.090	-0.230	-0.143	-0.112	-0.115
MSR(RE1)	0.056	-0.127	-0.205	0.048	0.006	0.052

Significant values ($p < 0.05$) are in bold

the northern and southern sections, it was observed that there were higher average reflectances in the Red-Edge/NIR region (Fig. 5). It was also noted that for the spectral region in Red-Edge/NIR, there were reflectance peaks for the month of February 2019 in both sections. However, average reflectances at RE2 (740 nm), RE3 (783 nm), NIR-8 (842 nm) and NIR-8a (865 nm) were higher in the northern area with no rust control. By analysing isolated bands, two SWIR bands were found to have the highest reflectance in December 2018, indicating a lower moisture content in the vegetation canopy.

Student's *t* test showed that the average reflectance of RE2 (B06), RE3 (B07), NIR-8 and NIR-8a bands in the

northern and southern sampling sections did not differ from each other in December 2018. However, reflectance averages became statistically different when comparing the north and south sample areas due to increased occurrence of coffee rust in January and February 2019, corresponding to higher reflectance in the northern section where the incidence of leaf rust was higher (Table 7).

The tested vegetation indices responded differently to rainfall intensity (Fig. 6). The curve of indices NDVI, NDMI(B11), NDMI(B12), RNDVI, NDVI(RE1), CI(RE1), MCARI/OSAVI and MSR(RE1) are similar and appeared to correspond with the rainfall intensity curve with a delay of

Fig. 5 Average monthly reflectance of Sentinel-2 spectral bands in the two areas (with and without coffee rust control measures) in the EPAMIG experimental fieldsite at Três Pontas city, Minas Gerais state, Brazil

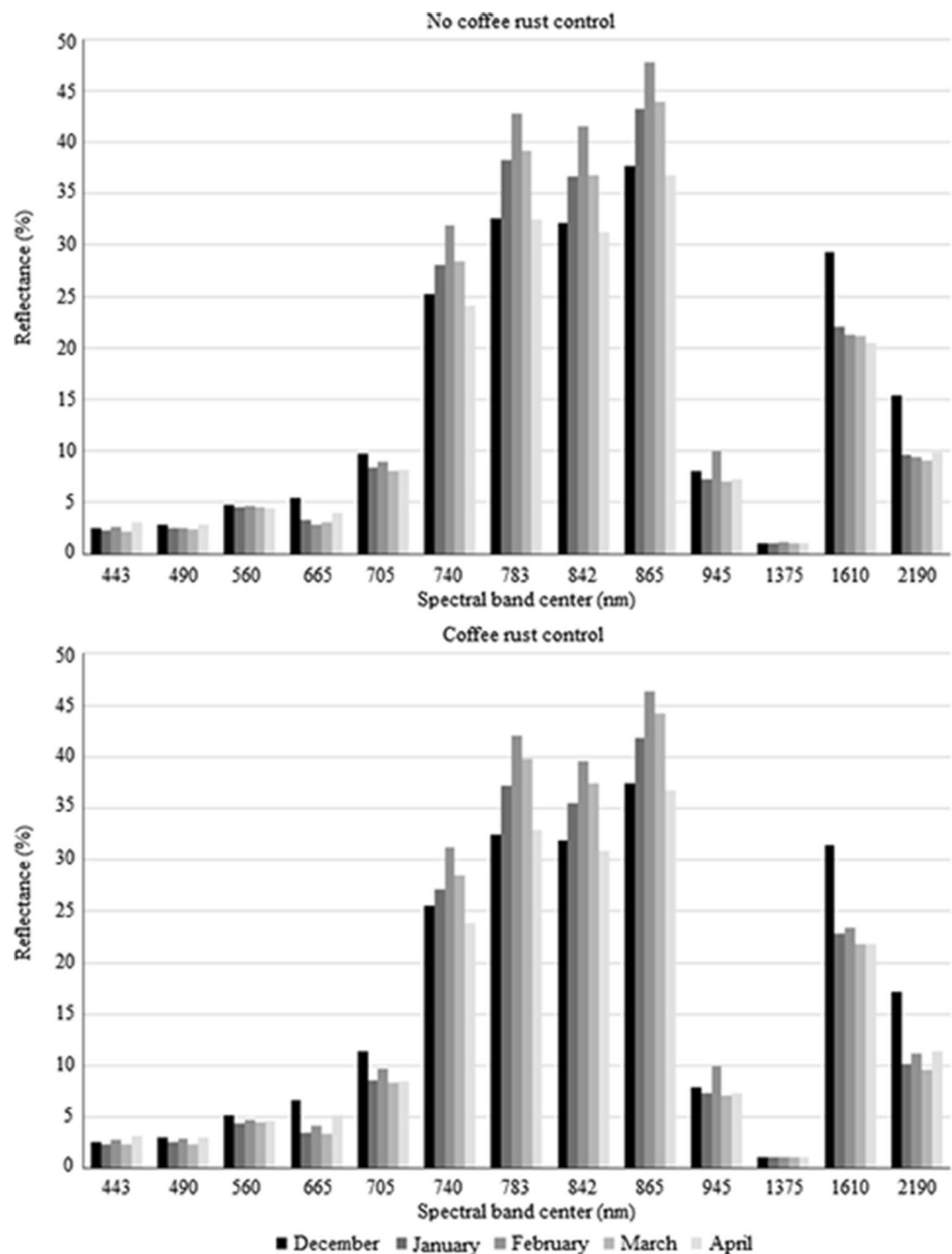


Table 7 Spectral bands reflectance averages of areas with (c) and without (nc) coffee rust control and Student's *t*-test results ('ns' equal to not significant) for independent samples (comparison of means)

Bands	Band center (nm)	December			January			February			March			April		
		Mean		<i>p</i> value	Mean		<i>p</i> value	Mean		<i>p</i> value	Mean		<i>p</i> value	Mean		<i>p</i> value
		c	nc		c	nc		c	nc		c	nc		c	nc	
B01	443	2.58	2.46	≤0.01	2.33	2.29	ns	2.76	2.64	≤0.01	2.29	2.21	≤0.01	3.13	3.08	ns
B02	490	3.07	2.79	≤0.05	2.52	2.48	ns	2.89	2.55	≤0.01	2.38	2.42	ns	3.08	2.90	ns
B03	560	5.12	4.75	≤0.05	4.35	4.50	≤0.01	4.77	4.60	ns	4.47	4.60	ns	4.57	4.49	ns
B04	665	6.70	5.41	≤0.01	3.50	3.30	≤0.05	4.17	2.88	≤0.01	3.33	3.05	ns	5.22	3.93	≤0.01
B05	705	11.42	9.70	≤0.01	8.58	8.41	≤0.05	9.67	8.92	≤0.01	8.30	8.02	≤0.05	8.45	8.19	ns
B06	740	25.50	25.21	ns	27.14	28.10	≤0.01	31.17	31.96	≤0.01	28.46	28.45	ns	23.86	24.16	≤0.05
B07	783	32.48	32.65	ns	37.18	38.19	≤0.01	42.07	42.73	≤0.01	39.83	39.14	≤0.01	32.86	32.44	ns
B08	842	31.90	32.11	ns	35.54	36.61	≤0.01	39.61	41.48	≤0.01	37.46	36.75	≤0.01	30.91	31.19	ns
B8a	865	37.45	37.67	ns	41.84	43.17	≤0.01	46.35	47.73	≤0.01	44.25	43.85	ns	36.81	36.75	ns
B09	945	7.89	8.01	≤0.01	7.28	7.28	ns	9.98	9.93	ns	7.08	7.05	ns	7.31	7.30	ns
B10	1375	1.08	1.08	ns	1.05	1.05	ns	1.15	1.16	≤0.01	1.06	1.05	≤0.01	1.08	1.08	ns
B11	1610	31.44	29.29	≤0.01	22.80	22.11	≤0.01	23.35	21.29	≤0.01	21.82	21.11	≤0.01	21.83	20.47	≤0.05
B12	2190	17.14	15.42	≤0.01	10.15	9.62	≤0.01	11.16	9.36	≤0.01	9.64	9.12	≤0.01	11.34	9.85	≤0.01

around 3 months, however, with different intensities. For indices calculated with SWIR bands, the pattern was observed more sharply. The vegetation index TCARI/OSAVI presented this same pattern in inverted form. For the IRECI case, the response to rainfall seemed to be faster, following the rainfall intensity curve with an interval of less than 1 month.

4 Discussion

This study aimed to evaluate the effectiveness of different vegetation indices calculated from Sentinel-2 MSI images for remote detection of coffee rust incidence symptoms, and to characterize the spectral signature of crops with different coffee rust incidence levels. Field data were obtained for comparative analysis with orbital data on several dates. Rainfall intensity data were estimated for the crop area to help understand the spectral behaviour of coffee plants with different disease intensity.

4.1 Spatial-temporal leaf rust distribution

Outbreaks of coffee rust were detected at the start of field evaluations, and from these affected spots the area that had not received chemical control was further infected by the disease. *Hemileia vastatrix* uredospores are dispersed inside the canopy by raindrops, through the spread of water flow in the infected leaves during rainfall [34]. In short, the sudden increase in the magnitude of disease incidence is the result of its effective dispersal through water [6, 38]. However, wind gusts also promote

uredospore dispersal across crops in full sun. Such dispersion is favoured during dry days with low relative humidity [7]. As a result, through the kriging map analysis it was observed that distribution and incidence intensity of coffee leaf rust were not homogeneous throughout the coffee field [2].

4.2 Correlation of data derived from Sentinel 2 with field data

Vegetation indices for remote disease monitoring may aid crop management. Through correlations between vegetation indices and field data for the same month, it was found that February 2019 is the best month to extract information on conditions of *H. vastatrix* infestation in coffee crops. In addition, it seemed appropriate to use vegetation indices that make use of bands in the NIR/Red-Edge region. Spectral bands positioned in the Red-Edge region appear to have greater sensitivity for identifying changes in the plant canopy when dealing with leaf diseases [9, 13, 18, 50].

The IRECI vegetation index calculated using MSI Sentinel-2 images from August and September 2018 was positively correlated with the February 2019 rust incidence data (IRECIaug $r=0.566$ and IRECIsep $r=0.493$). This observation may help in the localized control of coffee leaf rust, since in the subareas with higher IRECI values, higher levels of leaf rust incidence were observed. Furthermore, coffee leaf rust incidence data from April 2019 correlated positively with yield data collected in July 2019. The positive relationship between plant yield and coffee rust incidence

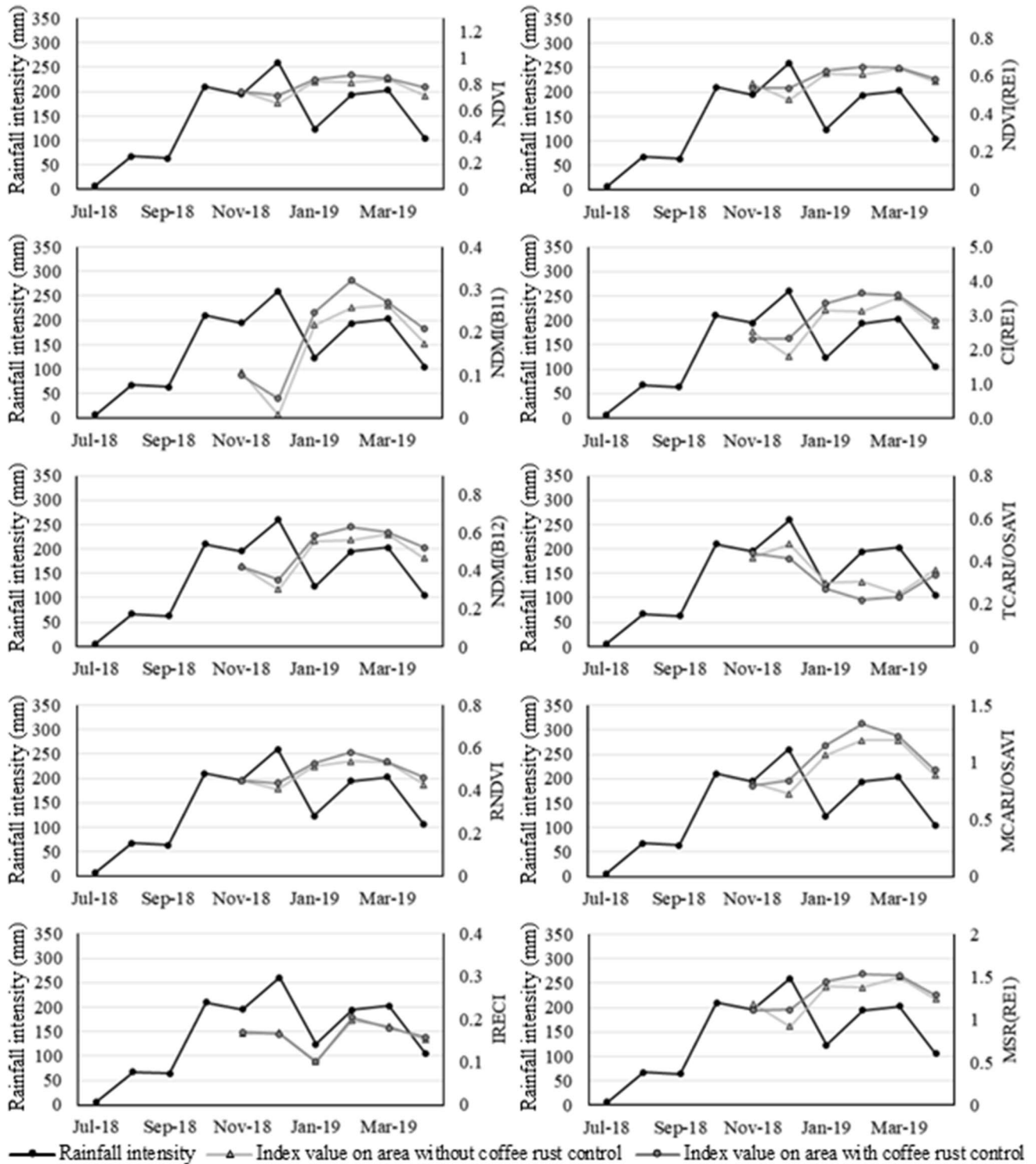


Fig. 6 Rainfall intensity and vegetation index curves of monthly mean values in areas with and without chemical control of coffee leaf rust at Três Pontas city, Minas Gerais state, Brazil

has been widely discussed in the specialized literature [4, 5, 8, 10, 16, 37, 43, 48].

4.3 Reflectance and vegetation index averages in areas with and without leaf rust control

This study reported higher average reflectances in the area with chemical control measures in February 2019 for bands RE2, RE3 and the two NIR plateau bands, relative to the area without chemical control. According to Knippling [33], reflectance in the NIR region is a result of the scattering of electromagnetic radiation that occurs due to existing interface areas in the transition between cell walls. Furthermore, the mesophyll deterioration leads to the reduction of existing air cavities, with a consequent reduction of reflectance in the NIR region. However, the author also notes that at the beginning of the leaf senescence process, there is an increase in these interface areas due to the separation of adjacent cells, as well as the distancing of living cell content from cell walls. Therefore, February 2019 may have marked the beginning of the leaf senescence process, as evidenced by increased reflectance in the Red-Edge/NIR region, most notably in the northern field site (without chemical control) which had higher coffee leaf rust incidence.

High reflectance values were observed for bands in the SWIR region for both areas in December 2018. The wavelengths in the SWIR region are absorbed by water, meaning that when vegetation suffers from a water deficit, there is increased reflectance in the spectral bands positioned in this region of the electromagnetic spectrum [29, 31, 46]. Therefore, despite the rainfall regime beginning in October 2018, the leaf structure had not yet shown to have water at its maximum potential.

Vegetation indices apparently responded to rainfall after approximately three months, with the exception of IRECI, which appears to have responded in less than a month. IRECI provides information on the chlorophyll content of leaves at a ratio close to 1:1 g/m² and still works well as a leaf area index [22]. Decreasing leaf water potential leads to decreased chlorophyll content, as this pigment is sensitive to increased environmental stress, especially salinity and drought [25]. Therefore, there may be a relationship with the occurrence of this observed behaviour and more detailed studies are needed to obtain better understanding.

5 Conclusions

This study demonstrated the varying effectiveness of vegetation indices for remote detection of coffee rust signs and symptoms through correlation analyses of different

indices. Vegetation indices obtained through relationships between bands in the Red-Edge and Near Infra-Red regions were more sensitive to changes caused by coffee leaf rust. Sentinel-2 orbital data transformed by calculating the IRECI vegetation index for August and September may be useful for indicating areas for coffee rust field sampling, and could be used to determine appropriate disease control according to variation in incidence rates. Future studies should examine the applicability of this vegetation index as a useful tool to aid in coffee plantation management.

Through this work it was also possible to characterize areas with different levels of disease incidence. The relationships between the monthly average spectral signature and levels of leaf rust incidence vary depending on the different regions of the electromagnetic spectrum. This may be due to the fact that the onset of the leaf senescence process reflectance peaks in most bands in the Red-Edge/NIR region were higher in areas with higher incidence of coffee leaf rust.

Acknowledgements The authors would like to thank the Coordenação de Aperfeiçoamento de Pessoal de Nível Superior (CAPES) (88882.446773/2019-01), Conselho Nacional de Desenvolvimento Científico e Tecnológico (CNPq) for the productivity Scholarship (GRC), and Empresa de Pesquisa Agropecuária de Minas Gerais (EPAMIG), Fundação de Amparo à Pesquisa do Estado de Minas Gerais (FAPEMIG), Universidade Federal de Lavras (UFLA) and José Luis Tavares Cortez for supporting this study.

Authors' contribution MLJC, MCA and GRC conceived and designed this research. MLJC conducted experiments. MLJC analysed data. MLJC wrote the manuscript. MCA, GRC and EAP reviewed and contributed to the writing of the article. All authors read and approved the manuscript.

Funding This study was funded by the Coordination for the Improvement of Higher Education Personnel (CAPES) (Process Number: 88882.446773/2019-01), supported by the Minas Gerais Agricultural Research Corporation (EPAMIG) and the Federal University of Lavras.

Availability of data and materials Data are available.

Code availability Free software were used.

Compliance with ethical standards

Conflict of interest On behalf of all authors, the corresponding author states that there is no conflict of interest.

Consent to participate All authors declare that they are aware of their participation in the present work.

Consent for publication All authors declare that they are aware of the submission of this work.

References

- Alvares CA, Stape JL, Sentelhas PC, de Moraes G, Leonardo J, Sparovek G (2013) Köppen's climate classification map for Brazil. *Meteorol Z* 22:711–728. <https://doi.org/10.1127/0941-2948/2013/0507>
- Alves MC, da Silva FM, Pozza EA, de Oliveira MS (2009) Modeling spatial variability and pattern of rust and brown eye spot in coffee agroecosystem. *J Pest Sci* 82:137–148. <https://doi.org/10.1007/s10340-008-0232-y>
- Auernhammer H (2001) Precision farming—the environmental challenge. *Comput Electron Agric* 30:31–43. [https://doi.org/10.1016/S0168-1699\(00\)00153-8](https://doi.org/10.1016/S0168-1699(00)00153-8)
- Avelino J, Willocquet L, Savary S (2004) Effects of crop management patterns on coffee rust epidemics. *Plant Pathol* 53:541–547. <https://doi.org/10.1111/j.1365-3059.2004.01067.x>
- Avelino J, Zelaya H, Merlo A, Pineda A, Ordóñez M, Savary S (2006) The intensity of a coffee rust epidemic is dependent on production situations. *Ecol Model* 197:431–447. <https://doi.org/10.1016/j.ecolmodel.2006.03.013>
- Bock KR (1962) Dispersal of uredospores of *Hemileia vastatrix* under field conditions. *Trans Br Mycol Soc* 45:63–74. [https://doi.org/10.1016/S0007-1536\(62\)80035-7](https://doi.org/10.1016/S0007-1536(62)80035-7)
- Boudrot A, Pico J, Merle I, Granados E, Vilchez S, Tixier P, Virginio-Filho EM, Casanoves F, Tapia A, Allinne C, Rice RA, Avelino J (2016) Shade effects on the dispersal of airborne *Hemileia vastatrix* uredospores. *Phytopathology* 106:572–580. <https://doi.org/10.1094/PHYTO-02-15-0058-R>
- Carvalho VL, Chalfoun SM, Castro HA, Carvalho VD (2001) Influence of different yield levels on coffee rust evolution and on phenolic compounds on leaves. *Cienc Agrotecnol* 25:49–54
- Coops N, Stanford M, Old K, Dudzinski M, Culvenor D, Stone C (2003) Assessment of *Dothistroma* needle blight of *Pinus radiata* using airborne hyperspectral imagery. *Phytopathology* 93:1524–1532. <https://doi.org/10.1094/PHYTO.2003.93.12.1524>
- Costa MJ, Zambolim L, Rodrigues FA (2006) Effect of levels of coffee berry removals on the incidence of rust and on the level of nutrients, carbohydrates and reductor sugar. *Fitopatol Bras* 31:564–571. <https://doi.org/10.1590/S0100-41582006000600005>
- Chavez PS Jr (1988) An improved dark-object subtraction technique for atmospheric scattering correction of multispectral data. *Remote Sens Environ* 24:459–479. [https://doi.org/10.1016/0034-4257\(88\)90019-3](https://doi.org/10.1016/0034-4257(88)90019-3)
- Chavez PS Jr (1989) Radiometric calibration of Landsat Thematic Mapper multispectral images. *Photogramm Eng Remote Sens* 55:1285–1294
- Chemura A, Mutanga O, Dube T (2017) Separability of coffee leaf rust infection levels with machine learning methods at Sentinel-2 MSI spectral resolutions. *Precis Agric* 18:859–881. <https://doi.org/10.1007/s11119-016-9495-0>
- Chen JM (1996) Evaluation of vegetation indices and a modified simple ratio for boreal applications. *Can J Remote Sens* 22:229–242. <https://doi.org/10.1080/07038992.1996.10855178>
- Custódio AAP, Pozza EA, Custódio AAP, Souza PE, Lima LA (2010) Effects of sun exposition on rust and cercospora leaf spot intensity on coffee plants. *Coffee Sci* 5:214–228
- Custódio AAP, Pozza EA, Custódio AAP, Souza PE, Lima LA, Silva AM (2014) Effect of center-pivot irrigation in the rust and brown eye spot of coffee. *Plant Dis* 98:943–947. <https://doi.org/10.1094/PDIS-07-13-0801-RE>
- Daughtry CST, Walthall CL, Kim MS, De Colstoun EB, McMurtrey JE III (2000) Estimating corn leaf chlorophyll concentration from leaf and canopy reflectance. *Remote Sens Environ* 74:229–239. [https://doi.org/10.1016/S0034-4257\(00\)00113-9](https://doi.org/10.1016/S0034-4257(00)00113-9)
- Eitel JU, Vierling LA, Litvak ME, Long DS, Schulthess U, Ager AA, Krofcheck DJ, Stoscheck L (2011) Broadband, red-edge information from satellites improves early stress detection in a New Mexico conifer woodland. *Remote Sens Environ* 115:3640–3646. <https://doi.org/10.1016/j.rse.2011.09.002>
- Empresa Brasileira de Pesquisa Agropecuária (1999) Controle da ferrugem o cafeeiro (*Hemileia vastatrix*) no estado de Rondônia. EMBRAPA. <https://ainfo.cnptia.embrapa.br/digital/bitstream/item/76700/1/FOL-7730-0001.pdf>. Accessed 15 Oct 2019
- European Space Agency (2015) Sentinel-2 user handbook. https://sentinel.esa.int/documents/247904/685211/Sentinel-2_User_Handbook. Accessed 17 Nov 2019
- Ferreira LG, Ferreira NC, Ferreira ME (2008) Sensoriamento remoto da vegetação: evolução e estado-da-arte. *Acta Sci Biol Sci* 30:379–390. <https://doi.org/10.4025/actasciobiolsci.v30i4.5868>
- Frampton WJ, Dash J, Watmough G, Milton EJ (2013) Evaluating the capabilities of Sentinel-2 for quantitative estimation of biophysical variables in vegetation. *ISPRS J Photogramm* 82:83–92. <https://doi.org/10.1016/j.isprsjprs.2013.04.007>
- Gitelson A, Merzlyak MN (1994) Quantitative estimation of chlorophyll-a using reflectance spectra: experiments with autumn chestnut and maple leaves. *J Photochem Photobiol B* 22:247–252. [https://doi.org/10.1016/1011-1344\(93\)06963-4](https://doi.org/10.1016/1011-1344(93)06963-4)
- Gitelson AA, Vina A, Ciganda V, Rundquist DC, Arkebauer TJ (2005) Remote estimation of canopy chlorophyll content in crops. *Geophys Res Lett* 32:1–4. <https://doi.org/10.1029/2005GL022688>
- Guerfel M, Baccouri O, Boujnah D, Chaïbi W, Zarrouk M (2009) Impacts of water stress on gas exchange, water relations, chlorophyll content and leaf structure in the two main Tunisian olive (*Olea europaea* L.) cultivars. *Sci Hortic* 119:257–263. <https://doi.org/10.1016/j.scienta.2008.08.006>
- Guimarães PTG, Garcia AWR, Alvarez VHA, Prezotti LC, Viana AS, Miguel AE, Malavolta E, Corrêa JB, Lopes AS, Nogueira FD, Monteiro AVC, Oliveira JA (1999) Cafeeiro. In: Ribeiro AC, Guimarães PTG, Alvarez VHA (eds) *Recomendações para o uso de corretivos e fertilizantes em Minas Gerais - 5ª Aproximação*. SBCS, Viçosa, pp 289–302
- Gürtler S, Epiphany JCN, Luiz AJB, Formaggio AR (2005) Electronic spreadsheet to acquire the reflectance from the TM and ETM + Landsat images. *Revista Brasileira de Cartografia* 57:162–167
- Huete A, Didan K, Miura T, Rodriguez EP, Gao X, Ferreira LG (2002) Overview of the radiometric and biophysical performance of the MODIS vegetation indices. *Remote Sens Environ* 83:195–213. [https://doi.org/10.1016/S0034-4257\(02\)00096-2](https://doi.org/10.1016/S0034-4257(02)00096-2)
- Hunt ER Jr, Rock BN, Nobel PS (1987) Measurement of leaf relative water content by infrared reflectance. *Remote Sens Environ* 22:429–435. [https://doi.org/10.1016/0034-4257\(87\)90094-0](https://doi.org/10.1016/0034-4257(87)90094-0)
- Instituto Nacional de Meteorologia. INMET. <http://www.inmet.gov.br/portal/index.php?r=estacoes/estacoesConvencionais>. Accessed 28 Oct 2019
- Jensen JR (2011) Sensoriamento remoto do ambiente: uma perspectiva em recursos terrestres. Parêntese, São José dos Campos
- Katsuhama N, Imai M, Naruse N, Takahashi Y (2018) Discrimination of areas infected with coffee leaf rust using a vegetation index. *Remote Sens Lett* 9:1186–1194. <https://doi.org/10.1080/2150704X.2018.1519269>
- Knipling EB (1970) Physical and physiological basis for the reflectance of visible and near-infrared radiation from vegetation. *Remote Sens Environ* 1:155–159. [https://doi.org/10.1016/S0034-4257\(70\)80021-9](https://doi.org/10.1016/S0034-4257(70)80021-9)
- Kushalappa AC, Eskes AB (1989) Resistance. In: Kushalappa AC, Eskes AB (eds) *Coffee rust: epidemiology, resistance and management*. CRC Press, Boca Raton, pp 171–292

35. Liaghat S, Balasundram SK (2010) A review: the role of remote sensing in precision agriculture. *Am J Agric Biol Sci* 5:50–55. <https://doi.org/10.3844/ajabssp.2010.50.55>
36. Lima PC (1979) Método de amostragem para a avaliação do índice de infecção da ferrugem do cafeeiro (*Hemileia vastatrix*, Berk. and Br.). Dissertation, Escola Superior de Agricultura “Luiz de Queiroz”
37. López-Bravo DF, Virginio-Filho EM, Avelino J (2012) Shade is conducive to coffee rust as compared to full sun exposure under standardized fruit load conditions. *Crop Prot* 38:21–29. <https://doi.org/10.1016/j.cropro.2012.03.011>
38. Nutman FJ, Roberts FM, Bock KR (1960) Method of uredospore dispersal of the coffee leaf-rust fungus, *Hemileia vastatrix*. *Trans Br Mycol Soc* 43:509–515. [https://doi.org/10.1016/S0007-1536\(60\)80033-2](https://doi.org/10.1016/S0007-1536(60)80033-2)
39. Pozza EA, Carvalho VL, Chalfoun SM (2010) Sintomas de injúrias causadas por doenças do cafeeiro. In: Guimarães RJ, Mendes ANG, Baliza DP (eds) *Semiologia do Cafeeiro*. Editora UFLA, Lavras, pp 67–106
40. Pires MSO, Alves MC, Pozza EA (2020) Multispectral radiometric characterization of coffee rust epidemic in different irrigation management systems. *Int J Appl Earth Obs* 86:102016. <https://doi.org/10.1016/j.jag.2019.102016>
41. Rondeaux G, Steven M, Baret F (1996) Optimization of soil-adjusted vegetation indices. *Remote Sens Environ* 55:95–107. [https://doi.org/10.1016/0034-4257\(95\)00186-7](https://doi.org/10.1016/0034-4257(95)00186-7)
42. Rouse Jr J, Haas RH, Schell, JA, Deering DW (1974) Monitoring vegetation systems in the Great Plains with ERTS. *Goddard Space Flight Center 3d ERTS-1 symposium, vol 1*, pp 309–317
43. Silva MG, Pozza EA, Vasco GB, Freitas AS, Chaves E, Paula PVAA, Dornelas GA, Alves MC, Silva MLO, Pozza AAA (2019) Geostatistical analysis of coffee leaf rust in irrigated crops and its relation to plant nutrition and soil fertility. *Phytoparasitica* 47:117–134. <https://doi.org/10.1007/s12600-019-00714-5>
44. United States Geological Survey. USGS. <https://earthexplorer.usgs.gov/>. Accessed 23 April 2019
45. Viola MR, de Mello CR, Pinto DB, de Mello JM, Ávila LF (2010) Spatial interpolation methods for mapping of rainfall. *Rev Bras Eng Agríc Ambient* 14:970–978. <https://doi.org/10.1590/S1415-43662010000900009>
46. Wilson EH, Sader SA (2002) Detection of forest harvest type using multiple dates of Landsat TM imagery. *Remote Sens Environ* 80:385–396. [https://doi.org/10.1016/S0034-4257\(01\)00318-2](https://doi.org/10.1016/S0034-4257(01)00318-2)
47. Wu C, Niu Z, Tang Q, Huang W (2008) Estimating chlorophyll content from hyperspectral vegetation indices: modeling and validation. *Agric For Meteorol* 148:1230–1241. <https://doi.org/10.1016/j.agrformet.2008.03.005>
48. Zambolim L, Silva-Acuña R, Do Vale FXR, Chaves GM (1992) Influência da produção do cafeeiro sobre o desenvolvimento da ferrugem (*Hemileia vastatrix*). *Fitopatol Bras* 17:32–35
49. Zambolim L (2016) Current status and management of coffee leaf rust in Brazil. *Trop Plant Pathol* 41:1–8. <https://doi.org/10.1007/s40858-016-0065-9>
50. Zheng Q, Huang W, Cui X, Shi Y, Liu L (2018) New spectral index for detecting wheat yellow rust using Sentinel-2 multispectral imagery. *Sensors* 18:868–887. <https://doi.org/10.3390/s18030868>

Publisher's Note Springer Nature remains neutral with regard to jurisdictional claims in published maps and institutional affiliations.